Erzincan Üniversitesi
Fen Bilimleri Enstitüsü Dergisi
2023, 16(3), 654-671
ISSN: 1307-9085, e-ISSN: 2149-4584
Araştırma Makalesi

Erzincan University
Journal of Science and Technology
2023, 16(3), 654-671
DOI: 10.18185/erzifbed.1352146
Research Article

Green Synthesis and Characterization of Silver Nanoparticles (AgNPs) and L-cysteine-capped AgNPs with *Foeniculum vulgare* seed extract for Colorimetric Hg^{2+} Detection

Deniz Uzunoğlu Doğruyol[1*]

[1]Department of Chemical Engineering, Mersin University, TURKEY

Received: 29/08/2022, **Revised**: 20/10/2023, **Accepted**: 20/10/2023**, Published**: 31/12/2023

Abstract

In this study, silver nanoparticles (AgNPs) and L-cysteine-capped AgNPs were synthesized separately using *Foeniculum vulgare* seed extract as the reducing agent and L-cysteine as the capping agent, which were characterized by ultraviolet–visible spectrophotometer (UV–vis), Fourier Transform Infrared spectrophotometer (FT-IR), X-ray diffractometer (XRD), and transmission electron microscopy (TEM). The utilization of the synthesized nanomaterials as colorimetric sensors for the detection of Hg^{2+} ions was also investigated. In this context, it was determined that L-cysteine-capped AgNPs exhibited better performance in the colorimetric Hg^{2+} detection in regards to sensitivity, selectivity, and applicability in real samples. It was observed that the colorimetric detection method was based on the disappearance of the brown color of the nanomaterial-contained colloidal solution and thus the decrease in the LSPR peak intensity. The method of the colorimetric Hg^{2+} detection with L-cysteine-capped AgNPs showed the good regression coefficient with the minimum detection limit of 0.36 µM in the linear Hg^{2+} concentration range of 1.0-10 µM, which indicated the competitive results compared to the latest reported colorimetric sensors in the literature. According to the obtained results, it has been concluded that the studied method enables to detection of Hg^{2+} ions colorimetrically via L-cysteine-capped AgNPs in a sensitive, selective, applicable in real samples, cheap, and easy way.

Keywords: L-cysteine-capped AgNPs, green synthesis, *Foeniculum vulgare*, Hg^{2+} detection, colorimetric sensor

Kolorimetrik Hg^{2+} Tespiti için *Foeniculum vulgare* Ekstraktı ile Gümüş Nanopartikülleri (AgNPs) ve L-sistein kaplı AgNPs'nin Yeşil Sentezi ve Karakterizasyonu

Öz

Bu çalışmada, indirgeyici ajan olarak *Foeniculum vulgare* ekstratı ve kaplayıcı ajan olarak L-sistein kullanılarak gümüş nanopartikülleri (AgNPs) ve L-sistein kaplı AgNPs ayrı ayrı sentezlenmiştir ve sentezlenen nanomalzemeler ultraviyole görünür spektrofotometre (UV-vis), Fourier Dönüşümlü Kızılötesi spektrofotometre (FT-IR), X-ışını difraktometre (XRD) ve transmisyon elektron mikroskobu (TEM) ile karakterize edilmiştir. Sentezlenen nanomalzemelerin Hg^{2+} iyonlarının tespiti için kolorimetrik sensör olarak kullanımı araştırılmıştır. Bu bağlamda, L-sistein kaplı AgNPs'nin kolorimetrik Hg^{2+} tespitinde duyarlılık, seçicilik ve gerçek örneklerde uygulanabilirlik açısından daha iyi performans gösterdiği belirlenmiştir. Kolorimetrik tespit yönteminin; nanomalzeme içeren koloidal çözeltinin kahverengi renginin kaybolmasına ve dolayısıyla LSPR pik şiddetinin azalmasına dayandığı gözlenmiştir. L-sistein kaplı AgNPs ile kolorimetrik Hg^{2+} tespit yöntemi, 1.0-10 µM doğrusal Hg^{2+} derişim aralığında 0.36 µM minimum saptama limiti ile iyi bir regresyon katsayısı göstermiştir ve bu da literatürde bildirilen güncel kolorimetrik sensörler ile rekabet edebilir sonuçlar elde edildiğine işaret etmiştir. Elde edilen sonuçlara göre; çalışılan yöntemin, L-sistein kaplı AgNPs ile Hg^{2+} iyonlarının kolorimetrik olarak hassas, seçici, gerçek numunelere uygulanabilir, ucuz ve kolay bir şekilde tespit edilmesine olanak sağladığı sonucuna varılmıştır.

Anahtar Kelimeler: L-sistein kaplı AgNPs, yeşil sentez, *Foeniculum vulgare*, Hg^{2+} tespiti, kolorimetrik sensor

*Corresponding Author: denizuzunoglu4@gmail.com
Yazar1 Deniz UZUNOĞLU DOĞRUYOL*, https://orcid.org/0000-0001-9706-303X

1. Introduction

Hg^{2+} is a stable toxic metal ion released to the environment from natural and anthropogenic sources which pollutes the environment and affects human health. Natural sources of mercury contain volcanic eruptions and emissions from the ocean while anthropogenic emissions are resulting from fuels or raw materials, or from uses in products or chemical, agricultural, and pharmaceutical industrial processes [1]. Mercury ion is regarded as a global public health risk due to its high-water solubility resulting to easily accumulation in water bodies. Thus, it gets into human body via water or food chain, passes through biological membranes, piles up in their physiological system, and leads to vital health problems including neurological, immunological, digestive, and cardiovascular diseases (Muhammad et al., 2022). The United States Environmental Protection Agency (USEPA) has specified the maximum permissible concentration of Hg^{2+} in drinking water as 10 nM, while it has been set as 30 nM by the world health organization (WHO) (Jayeoye et al., 2022). The development of high-sensibility analytical methods is needed for the detection and quantification of Hg^{2+} in water samples according to such low regulatory limits. It can be detected by conventional methods including atomic absorption/emission spectroscopy, electrochemical methods, X-ray fluorescence spectrometry, inductively coupled plasma mass spectroscopy, gas chromatography, and colorimetric assays [2]. Although high selectivity and sensitivity are provided by these methods, several disadvantages such as extensive sample pretreatments, complex instruments, and/or more samples limit their applicability [4]. Therefore, different types of sensors like colorimetric, electrochemical, fluorescence have been developed for the low-cost, sensitive, selective, and quick detection of Hg^{2+} in aqueous samples. Among the sensors, colorimetric sensors necessitate minimal instrumentation and so enable easier on-site detection. Especially metallic nanoparticles have attracted much attention due to their superior properties such as extremely high extinction coefficients and strongly distance-dependent optical properties, which allow being effective colorimetric sensors [5].

The principle of colorimetric detection with metallic nanoparticles is based on Localized Surface Plasmon Resonance (LSPR) phenomenon related to the collective oscillation of conduction electrons when interacting with visible light, which makes the metallic nanoparticle-contained colloidal solution has a characteristic color. Accordingly, an external intervention like adding heavy metal solution may alter the solution color and thus induce a shift in the LSPR absorption peak due to interparticle plasmon incorporation [6]. LSPR electrons on the surface of silver nanoparticles (AgNPs) result in the characteristic absorbance peak in the visible wavelength region between the range of 400-500 nm, which provides convenience in the colorimetric detection of Hg^{2+}. The colorimetric detection of Hg^{2+} with AgNPs is based on the redox reaction between Ag^{1+}/Ag^{0} (E^{0}=0.799 V) and Hg^{2+}/Hg^{0} (E^{0}=0.85 V), which leads to the loss of LSPR absorption peak and thus the decolorization of AgNPs-contained colloidal solution.

The reaction occurs by means of the superior properties of AgNPs such as solubility in water, unique optical properties, and stability, which aids the formation of silver–mercury amalgam [1, 7]. AgNPs have been widely synthesized by the chemical reduction method; however,

*Corresponding Author: denizuzunoglu4@gmail.com
Yazar1 Deniz UZUNOĞLU DOĞRUYOL*, https://orcid.org/0000-0001-9706-303X

natural sources such as plants, fungi, algae, yeast, bacteria have been used instead of the chemical reductants recently due to the high-cost of them.

Although effective Hg^{2+} detection has been made with AgNPs synthesized by chemical reduction method, the detection with green synthesized AgNPs has been proposed as a more eco-friendly and cost-effective method recently. There are many advantages of using plants in the green synthesis such as availability, no need for sterilization, simplicity, and safe to be processed of plants compared to other natural sources. For these reasons, the effective green synthesis of AgNPs with plant extract for Hg^{2+} detection under mild conditions is still in demand both environmentally and industrially [8].

Foeniculum vulgare contains proteins, fats, minerals, fibers, carbohydrates, and phytochemical compounds [9]. The phytochemical compounds such as amino acids, volatile compounds, fatty acid, and phenolics, flavonoids play important roles in reduction of silver ion (Ag^{1+}) to zero-valent silver (AgNPs) due to their strong antioxidant effects.

Surface modification improves the stability and analytical applicability of AgNPs for metal ion detection. Various compounds containing –SH, $–NH_2$, –COOH, and –OH functional groups such as polyvinyl alcohol [10], calixarene [11], thiol terminated chitosan [12], 3,4-dihydroxy-L-phenylalanine [13], Riboflavin, 1-dodecanethiol, starch, 2-aminopyrimidine-4,6-diol, citrate, L-tyrosine, glutathione, casein peptide, L-tyrosine, tartaric acid [14], L-cysteine [15], 3-mercapto-1,2-propanediol [16] have been applied as capping agents and as well as reducing agents.

In this work, *F. vulgare* seed extract was chosen as reducing agent and modification of AgNPs surface was carried out using L-cysteine. The characterization studies have been carried out with UV-vis spectrophotometer, FT-IR, XRD, and TEM analyses. The synthesized AgNPs and L-cysteine-capped AgNPs have been evaluated in the colorimetric detection of Hg^{2+}. In this content; the studies of the sensitivity, selectivity, and applicability in real samples have been carried out and also the effect of the use of L-cysteine on colorimetric Hg^{2+} detection has been discussed.

2. Material and Methods

2.1. Green Synthesis and Characterization of AgNPs and L-cysteine-capped AgNPs

For the synthesis of AgNPs and L-cysteine-capped AgNPs, the aqueous extract of *F. vulgare* seeds was firstly prepared. With this scope, *F. vulgare s*eeds were purchased from a herbalist in Mersin, Turkey. The purchased seeds were firstly rinsed with tap water and then washed with distilled water. After that, they were dried in an oven at 50 °C for 3.0 h. The aqueous extract of *F. vulgare* seeds was prepared by heating of 10 g of the seeds in 300 mL distilled water at 60 ^oC for 2.0 hours. The prepared aqueous extract was cooled to room temperature, and then the seeds were separated from the extract with Whatman #1 filter paper. Lastly, the prepared aqueous extract was stored in the refrigerator at +4 °C for further the nanomaterial synthesis experiments.

The as-prepared aqueous extract was then utilized as a reducing agent for reducing +1 valent silver ion ($AgNO_3$) to zero-valent silver (AgNPs). For the synthesis of both nanomaterials, 5.0

mL of the aqueous extract was added to 45 mL of 10 mM $AgNO_3$ solution. Differently from AgNPs, the desired amounts of L-cysteine were poured into the mixture for the synthesis of L-cysteine-capped AgNPs.
Lastly, the as-prepared mixtures were kept overnight at room temperature at dark. The mixtures, which changed color from yellow to brown overnight, were stored in the refrigerator at +4 °C to be used for the colorimetric detection [17].

The schematic illustration of L-cysteine-capped AgNPs formation was presented in Figure 1.

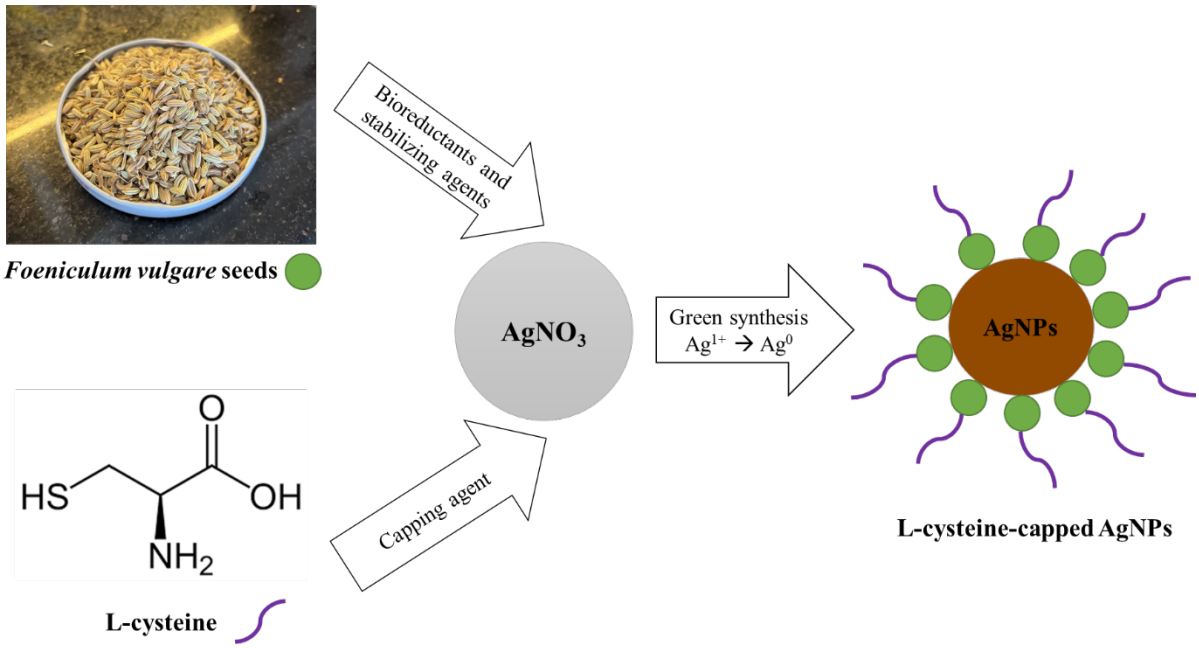

Figure 1. The schematic illustration of L-cysteine-capped AgNPs formation

The UV-vis spectroscopy measurements of the nanomaterials were recorded in a wavelength ranging from 300 to 800 nm for the observation of the LSPR absorption peak. The functional groups present in the nanomaterials were investigated using FTIR. The sizes and morphologies of the nanomaterials were performed by TEM. For the investigation of the crystal phases of the nanomaterials, XRD analysis was performed in 2θ value ranging from 20 ° to 80°.

2.2. Colorimetric Hg^{2+} Detection with AgNPs and L-cysteine-capped AgNPs

In conducting Hg^{2+} detection with the synthesized nanomaterials, 1.0 mL aliquot of the nanomaterial-contained colloidal solution and 1.5 mL of distilled water were added sequentially into an UV−vis spectrophotometer cuvette and its UV–vis absorbance spectrum was recorded as blank. The characteristic LSPR absorption peaks of AgNPs and L-cysteine-capped AgNPs were determined as 465 nm and 450 nm, respectively. After that, 1.5 mL of a certain concentration of Hg^{2+} solution was added to the mixture of 1.0 mL of nanomaterial-contained colloidal solution and 1.5 mL of distilled water, and the resulting solution was thoroughly mixed manually. The absorbance value of the mixture of 1.0 mL of nanomaterial-contained colloidal solution and 1.5 mL of distilled water was named A_0 while the absorbance value after adding of 1.5 mL of a certain concentration of Hg^{2+} solution was named A_1. A_1 values were recorded

5.0 minutes later after adding of 1.5 mL of a certain concentration of Hg^{2+} solution. The difference of these two absorbance values ($\Delta A=A_0-A_1$) was collected as experimental data.
The sensitivity of the procedure was tested by adding of 1.5 mL of Hg^{2+} solutions at different concentrations to each mixture of 1.0 mL of nanomaterial-contained colloidal solution and 1.5 mL of distilled water. In order to investigate the selectivity of the as-synthesized nanomaterials in detecting Hg^{2+}, 1.5 mL solutions of representative metals ions at 1000 μM concentration were each added to the mixture of 1.0 mL of nanomaterial-contained colloidal solution and 1.5 mL of distilled water. The color changes of the mixtures were observed with naked-eye and the corresponding absorbance changes were affirmed with the UV–vis spectrophotometer [1].

3. Results and Discussions

3.1. Characterization of AgNPs and L-cysteine-capped AgNPs

AgNPs and L-cysteine-capped AgNPs were synthesized in different proportions of the components as can be seen in Table 1. The characteristic LSPR absorption peaks of the synthesized nanomaterials were observed via UV-vis spectrophotometer and the related spectra were given in Figure 2. Accordingly, it was determined that the presence of more than 1.0 mL of L-cysteine in the medium at the constant volume of the aqueous extract caused the characteristic LSPR absorption peaks to disappear. It was also observed that the intense of the characteristic LSPR absorption peak was increased with increasing the amount of the aqueous extract, indicating the increase in the amount of the formed nanomaterial. Thus, the colorimetric Hg^{2+} detection experiments were performed with the nanomaterials synthesized at the proportions of a, b, e, and f. Then, the colorimetric Hg^{2+} detection performance of the nanomaterials decided to be studied was examined. Although nanomaterial formation was high at high aqueous extract volumes, it was decided to continue the detection experiments with the nanomaterials synthesized at the proportions of a and b since higher colorimetric detection efficiencies for especially Hg^{2+} concentration of 10^{-6} M were obtained with these nanomaterials.

Table 1. The proportions of the components in the synthesis of AgNPs and L-cysteine-capped AgNPs

Nanomaterial code	$AgNO_3$	Aqueous extract of *F. vulgare* seeds	L-cysteine	LSPR	Colorimetric detection efficiency (%)	
					For $2x10^{-4}$ M Hg^{2+}	For 10^{-6} M Hg^{2+}
a	10 mM, 45 mL	5.0 mL	-	465 nm	57.14	23.12
b	10 mM, 45 mL	5.0 mL	1.0 mM, 1.0 mL	450 nm	63.05	23.82
c	10 mM, 45 mL	5.0 mL	1.0 mM, 3.0 mL	-	-	-
d	10 mM, 45 mL	5.0 mL	1.0 mM, 5.0 mL	-	-	-
e	10 mM, 45 mL	10 mL	-	465 nm	45.72	2.12
f	10 mM, 45 mL	10 mL	1.0 mM, 1.0 mL	465 nm	51.12	3.84
g	10 mM, 45 mL	10 mL	1.0 mM, 3.0 mL	-	-	-
h	10 mM, 45 mL	10 mL	1.0 mM, 5.0 mL	-	-	-

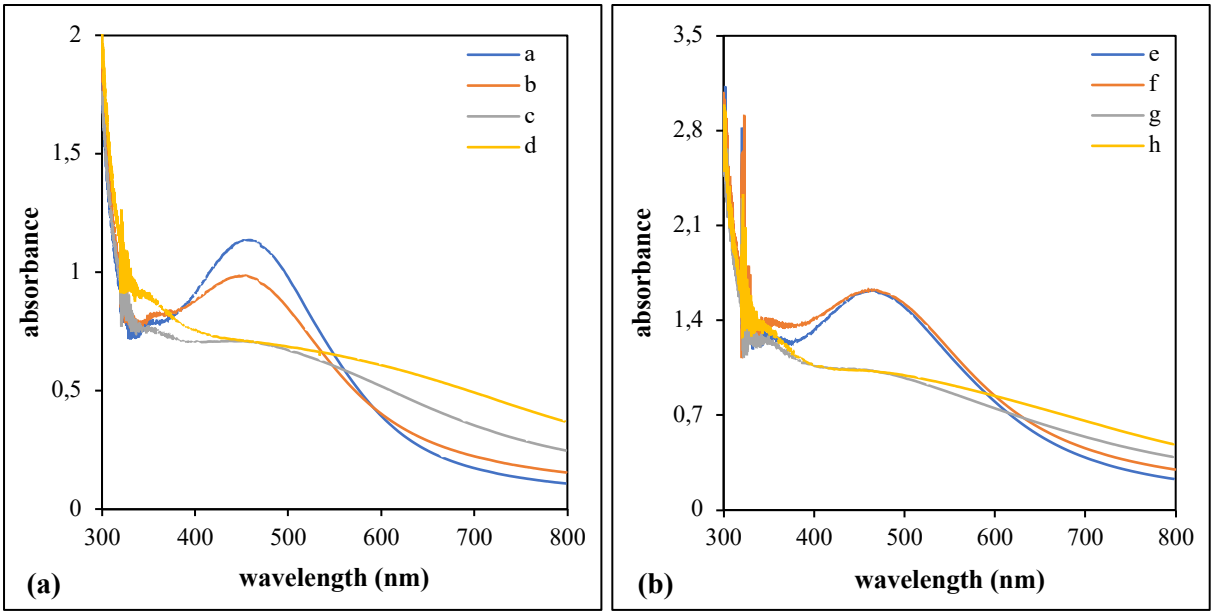

Figure 2. The UV-vis spectra of the synthesized nanomaterials in different proportions of the components **(a)** nanomaterial code: a-d, **(b)** nanomaterial code: e-h

The functional groups of the nanomaterials synthesized at the proportions of a and b were analyzed by FT-IR and the obtained spectra were presented in Figure 3. Accordingly, the spectra of L-cysteine-capped AgNPs exhibited a peak at 2250 cm^{-1}, related to the presence of mercaptans –SH. This peak for –SH was not observed in case of AgNPs, demonstrating the formation of S–Ag covalent interaction [18, 19]. Moreover, differently from AgNPs, L-cysteine-capped AgNPs showed a peak at 2979 cm^{-1} corresponding to $–NH_3^+$ stretching, a bending band of N–H at 1502 cm^{-1}, and two bands at 1620 and 1367 cm^{-1} related to the asymmetric and symmetric stretching of $COO^–$, respectively [19]. The peak at around 1600 cm^{-1} related to C=O stretching vibration. The peak at around 1300 cm^{-1} was related to the O-H bending and affirmed the presence of an aromatic group, while the absorption peak at around 1000 cm^{-1} originated from C-O-C and secondary -OH group. The aforementioned peaks, which were common to both nanomaterials, stemmed from the extract structure [5].

Figure 4 displayed XRD patterns of the nanomaterials synthesized at the proportions of a and b. The XRD patterns designated that the five characteristic diffraction peaks were obtained at $2\theta = 38^\circ, 44^\circ, 64^\circ, 77^\circ$, and 81°, which can be indexed to (111), (200), (220), (311), and (222) planes of the face-centered-cubic structure of silver nanoparticles [19]. The sharpness of reflection peaks proves the crystallinity level of the materials; accordingly, L-cysteine-capped AgNPs had higher crystallinity than AgNPs due to its sharper reflection peaks [20].

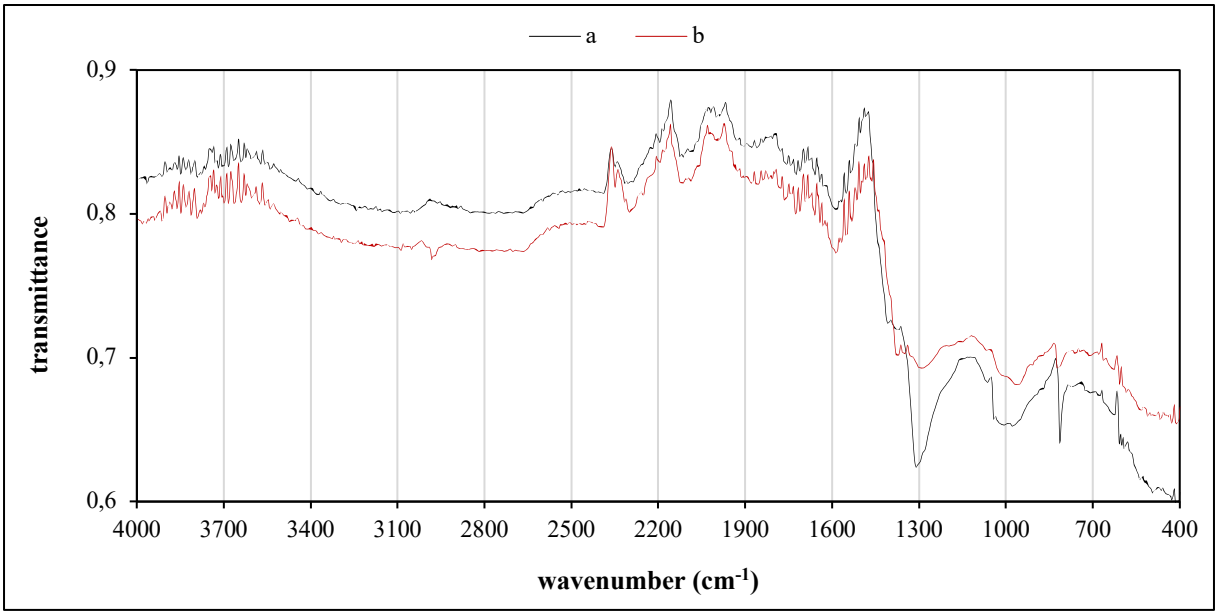

Figure 3. FT-IR spectra of the nanomaterials synthesized at the proportions of a and b

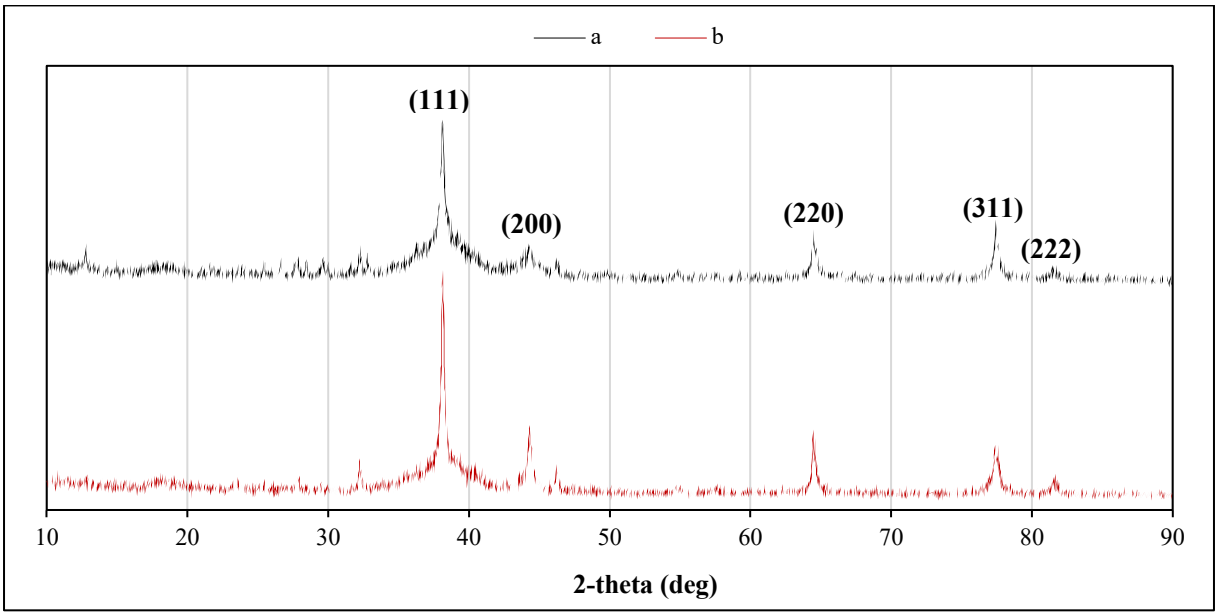

Figure 4. XRD patterns of the nanomaterials synthesized at the proportions of a and b

The morphological characteristics were evaluated using TEM analysis and the obtained TEM images for the nanomaterials synthesized at the proportions of a and b were presented in Figure 5 (a) and (b), respectively. Randomly selecting 25 particles from TEM images with the Image J program, the particle sizes of AgNPs and L-cysteine-capped AgNPs were calculated to be 11.84±1.92 nm and 7.82±1.20 nm, respectively. Accordingly, less agglomeration and lower particle size were observed in the TEM image of L-cysteine-capped AgNPs. The enhanced monodispersity could be ascribed to the capping of L-cysteine on the surface of Ag NPs, which was further affirmed by the peak for –SH in FT-IR spectra of L-cysteine-capped AgNPs.
TEM images of the nanomaterials synthesized at the proportions of a and b after Hg^{2+} detection were given in Figure 5 (c) and (d), respectively.

Randomly selecting 25 particles from TEM images with the Image J program, the particle sizes of AgNPs and L-cysteine-capped AgNPs after Hg^{2+} detection were obtained as 12.71±2.43 nm and 10.49±1.62 nm, respectively. The related figures showed that the nanomaterials agglomerated and so their sizes increased after the colorimetric detection reaction between Ag^{1+}/Ag^0 and Hg^{2+}/Hg^0 due to the formation of solid like an amalgam of silver and mercury.

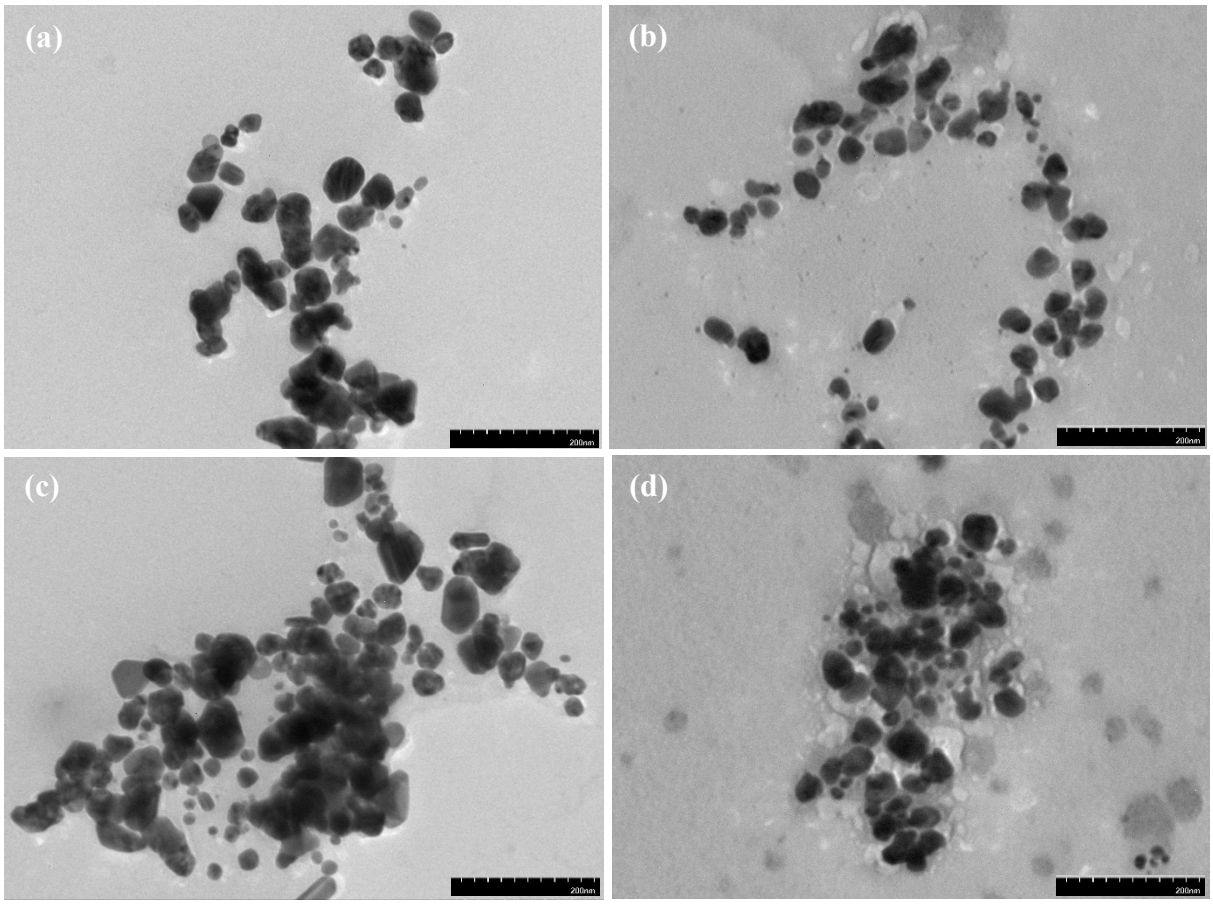

Figure 5. TEM images of the nanomaterials synthesized at the proportions of a and b, (c) and (d) TEM images of the nanomaterials synthesized at the proportions of a and b after Hg^{2+} detection, respectively

3.2. Colorimetric Hg^{2+} Detection with AgNPs and L-cysteine-capped AgNPs

The colorimetric Hg^{2+} detection performances of AgNPs and L-cysteine-capped AgNPs were presented in Figure 6 (a) and (b), respectively. The characteristic LSPR absorption peaks of AgNPs and L-cysteine-capped AgNPs were determined as 465 nm and 450 nm, respectively. The addition of Hg^{2+} ions led to remarkable decreases of the LSPR absorption peaks and decolorization of the solutions from brown to colorless, enabling the colorimetric detection of Hg^{2+} via the redox reaction between Ag^{1+}/Ag^0 (E^0=0.799 V) and Hg^{2+}/Hg^0 (E^0=0.85 V). The color change was evaluated a visual output, and the absorbance difference in the LSPR peak was used as experimental data in the colorimetric Hg^{2+} detection system. Accordingly, the absorbance difference in the LSPR peak of L-cysteine-capped AgNPs (ΔA=0.67) was higher than that of AgNPs (ΔA=0.62), indicating that L-cysteine-capped AgNPs could be used as a more effective sensor for the colorimetric Hg^{2+} detection.

The proposed detection mechanism was resulting from Hg^{2+} induced-deprotection followed by spontaneous oxidation of Ag^0. When Hg^{2+} ions were added to L-cysteine-capped AgNPs-contained colloidal solution, they interfered the interaction of AgNPs and L-cysteine and carboxyl or hydroxyl groups in the extract. L-cysteine and the functional groups in the extract provided capping and stabilizing the AgNPs during the synthesis process. These capping and stabilizing groups were separated from AgNPs due to the strong affinity of Hg^{2+}, resulting in the destabilization of AgNPs. Then, Hg^{2+} spontaneously oxidized the destabilized-AgNPs as it had a higher reduction potential than Ag^{1+}. The oxidation of AgNPs caused the disappearance of LSPR absorption peak, as well as the decolorization of L-cysteine-capped AgNPs-contained colloidal solution [6]. This proposed detection mechanism of Hg^{2+} with L-cysteine-capped AgNPs was illustrated in Figure 7.

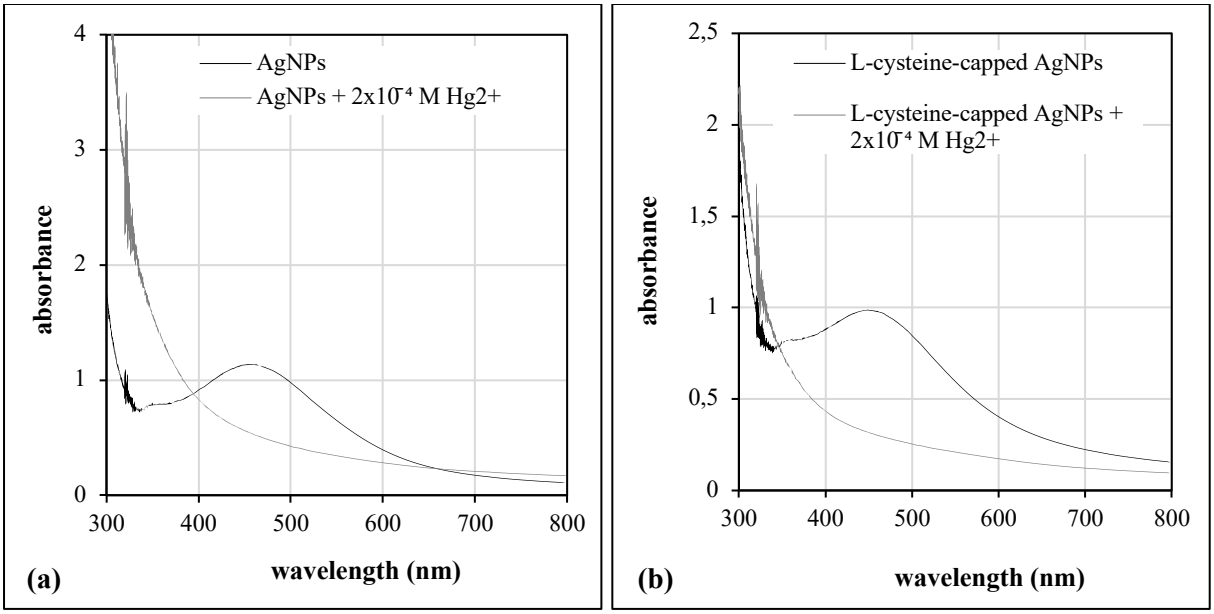

Figure 6. The colorimetric Hg^{2+} detection performance of **(a)** AgNPs and **(b)** L-cysteine-capped AgNPs

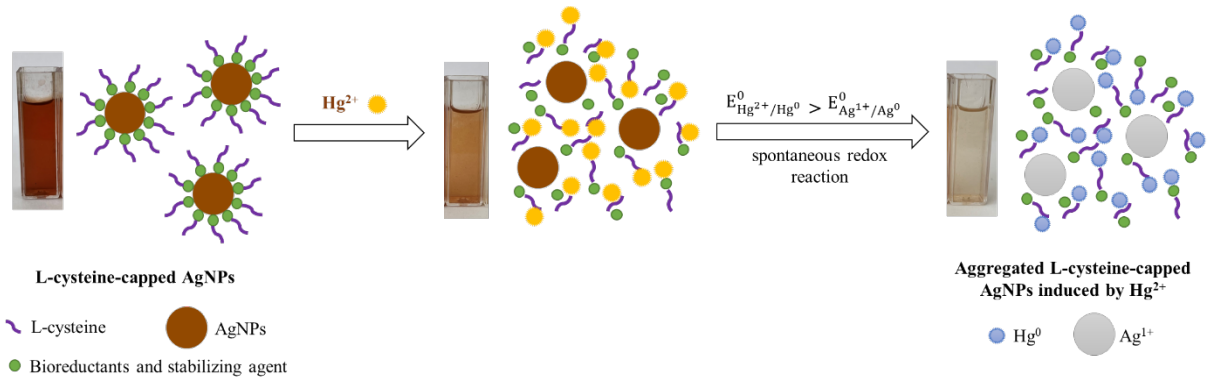

Figure 7. The proposed detection mechanism of Hg^{2+} with L-cysteine-capped AgNPs

The limit of detection (LOD) is important for colorimetric sensors, that is used for distinguishing the detection method as well as explicating the experimental data. In order to determine the LOD value of AgNPs and L-cysteine-capped AgNPs for the colorimetric Hg^{2+} detection, calibration lines were created by plotting the different Hg^{2+} concentrations versus the absorbance differences ($\Delta A=A_0-A_1$) at these concentrations. The changes of absorbance differences with Hg^{2+} concentrations for AgNPs and L-cysteine-capped AgNPs were presented in Figure 8 (a) and (b), respectively. Accordingly, two linear portions in the ranges of 1.0–10 µM (ΔA = 10855C+0.2185, R^2 = 0.901 for AgNPs; ΔA=17805C+0.2384, R^2=0.9047 for L-cysteine-capped AgNPs) and 20–400 µM (ΔA=1247.8C+0.347, R^2=0.9697 for AgNPs; ΔA=1377.6C + 0.406, R^2=0.9683 for L-cysteine-capped AgNPs) were obtained, where C was the Hg^{2+} concentration in molar. The limit of detection (LOD= 3σ/s) was calculated in regard to the signal which was equivalent to 3 times the standard deviation of the blanks, where s was the slope of the calibration line in the Hg^{2+} concentration range of 1.0–10 µM and σ was the standard deviation of the control solution. Accordingly, LOD values of AgNPs and L-cysteine-capped AgNPs were obtained to be 1.58 µM and 0.36 µM, respectively. The LOD values of the synthesized nanomaterials were compared with the AgNPs in the latest reported works as can be seen in Table 2. The literature survey indicated that L-cysteine-capped AgNPs exhibited relatively competitive Hg^{2+} colorimetric sensing activity when compared to the AgNPs in the latest reported works.

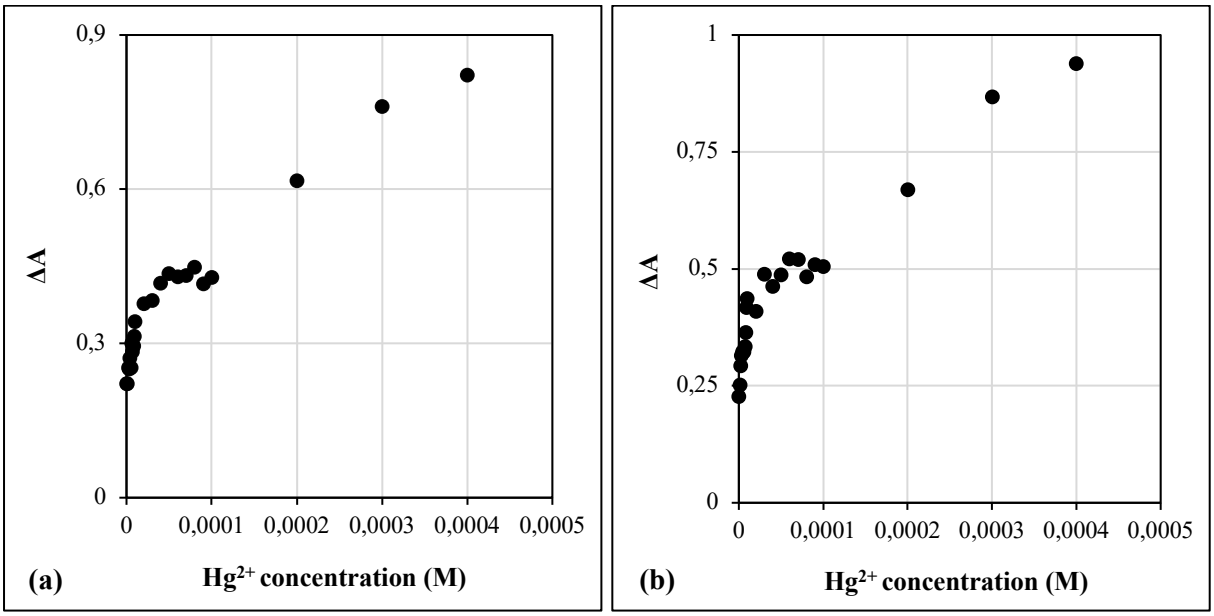

Figure 8. The changes of absorbance differences with Hg^{2+} concentrations for **(a)** AgNPs and **(b)** L-cysteine-capped AgNPs

Table 2. The comparison of linear ranges and LOD values of AgNPs and L-cysteine-capped AgNPs with the previously reported AgNPs

Colorimetric sensor	Synthesis method	LOD value	Linear range	Reference
Ziziphus mauritiana Leaf extract-based silver nanoparticles	Green synthesis	0.04 nM	3–23 nM	[21]
Lignosulfonate capped silver nanoparticles	Chemical reduction	7 nM	0–68 μM	[22]
L-cysteine modified silver nanoparticles	Chemical reduction	8 nM	0.04-1.04 μM	[23]
Cysteine capped silver nanoparticle	Chemical reduction	45.39 nM	1–2500 nM	[24]
Carboxylic Acid-Capped Silver Nanoparticles	Chemical reduction	0.12 μM	0.6–1.6 μM	[25]
Triazole stabilized silver nanoparticles	Chemical reduction	0.33 μM	1–100 μM	[26]
L-cysteine-capped AgNPs	Green synthesis	0.36 μM	1.0–10 μM	This work
Orange Peel-mediated silver nanoparticles	Green synthesis	1.24 μM	1–100 μM	[1]
Gingerol extract-stabilized silver nanoparticles	Green synthesis	1.46 μM	0–160 mM	[27]
AgNPs	Green synthesis	1.58 μM	1.0–10 μM	This work
N-(3,5-bis(trifluoromethyl)phenyl)-2-(4-chlorophenyl) Hydrazine Carbothioamide-AgNPs	Chemical reduction	2.2 μM	4–68.4 μM	[2]
Citrate-γ-aminobutyric acid@AgNPs	Chemical reduction	2.37 μM	5–35 μM	[28]
Chlorophyll functionalized silver nanoparticles	Green synthesis	2.7 μM	50 nM-500 μM	[29]
Acacia confusa leaf-mediated AgNPs	Green synthesis	44.3 μM	0-50 μM	[30]

The binding stoichiometries of Hg^{2+} and the synthesized nanomaterials were evaluated by continuous variation analysis via Job's plot. In the Job's plot, the absorbance differences vary with molar ratios of Hg^{2+} and the synthesized nanomaterials while the total molar concentration remains constant. Job's plot proposes 1:1 stoichiometry between the reactants (Hg^{2+} and the synthesized nanomaterials for this study) by molar ratio of 0.5, where the maximum binding is achieved. The binding stoichiometries of Hg^{2+} and the synthesized nanomaterials were analyzed by the graph plotted between $1/(A_0-A_1)$ versus $1/[Hg^{2+}]$, depending upon the Benesi–Hildebrand Equation given below [31]:

$$\frac{1}{(A_o - A_1)} = \frac{1}{(A_f - A_o)} + \frac{1}{(A_f - A_o).K_{a.c}.[Hg^{2+}]} \quad (1)$$

where A_o, A_1, and A_f are absorbances of Hg^{2+}–the synthesized nanomaterials at 450 nm for AgNPs and at 465 nm for L-cysteine-capped AgNPs, at each added Hg^{2+} concentration, and at infinite Hg^{2+} concentration, respectively, whereas $[Hg^{2+}]$ and $K_{a.c}$ are various added Hg^{2+} concentrations and association constant, respectively. The good linear relationships based on the Benesi–Hildebrand Equation were presented in Figure 9 (a) and (b) for AgNPs and L-cysteine-capped AgNPs, respectively. Accordingly, the association constants for Hg^{2+}–AgNPs complex and Hg^{2+}–L-cysteine-capped AgNPs complex were determined as 242.887x10^3 M^{-1} and 226.112x10^3 M^{-1}, respectively. The obtained $K_{a.c}$ values indicated that AgNPs exhibited better bonding affinity to Hg^{2+} ions than L-cysteine-capped AgNPs.

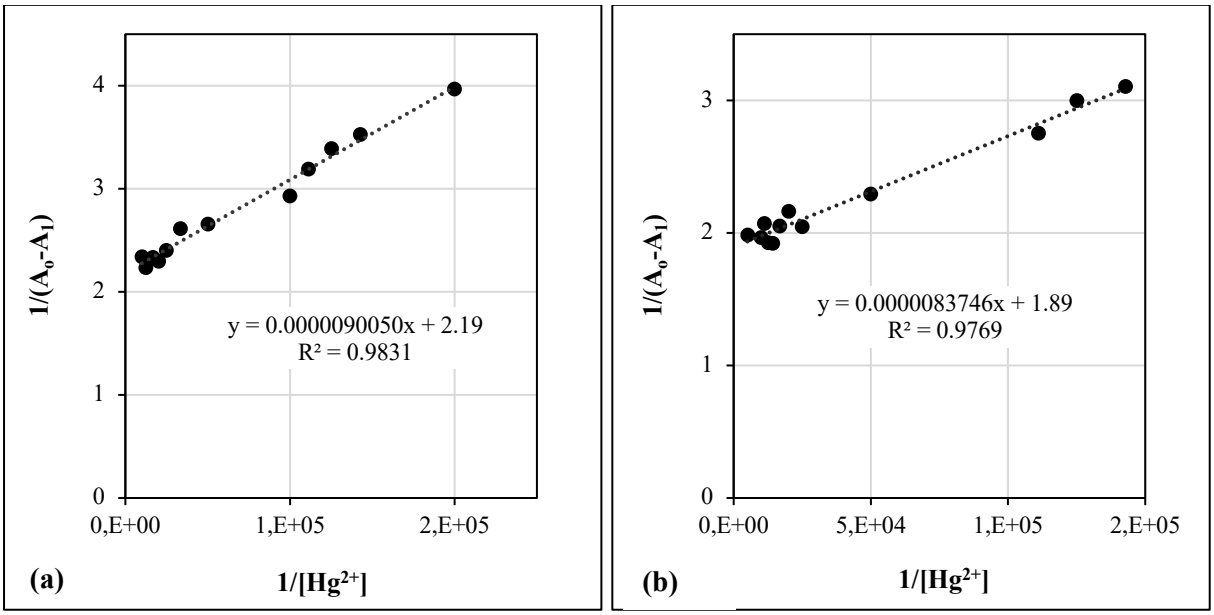

Figure 9. The linear relationship based on the Benesi–Hildebrand Equation for the formation of **(a)** Hg^{2+}–AgNPs complex and **(b)** Hg^{2+}– L-cysteine-capped AgNPs complex

In order to investigate the selectivity of the synthesized nanomaterials for the detection of Hg^{2+}, 1.5 mL solutions of the representative metal cations were each added to the mixture of 1.0 mL of nanomaterial-contained colloidal solution and 1.5 mL of distilled water. The Hg^{2+} concentration was maintained at 100 µM whereas other metal cations were at 1000 µM. The color changes were observed with the naked-eye and the corresponding absorbance differences were affirmed with the UV–vis spectrophotometer. The corresponding absorbance differences and the recovery values were given in Figure 10 and Table 3, respectively.

The recovery values were calculated with Equation 2 given below:

$$\text{Recovery \%} = \frac{\Delta A_i}{\Delta A_r} \text{ x } 100 \qquad (2)$$

where A_i is the absorbance change in the presence of the metal cation i, A_r is the absorbance change in the presence of reference that is distilled water.

As shown in Figure 10 (a) and (b), the highest absorbance differences were observed for only the addition of Hg^{2+} ion even when other metal cations were at ten-fold concentration higher than Hg^{2+}. Moreover, as seen in Table 3, the recovery values for metal cations were between 89.32 % and 97.54 % for AgNPs while they were between 91.21 % and 101.80 % for L-cysteine-capped AgNPs. These results showed that L-cysteine-capped AgNPs could be more effectively utilized in the colorimetric Hg^{2+} detection in the presence of various metal cations.

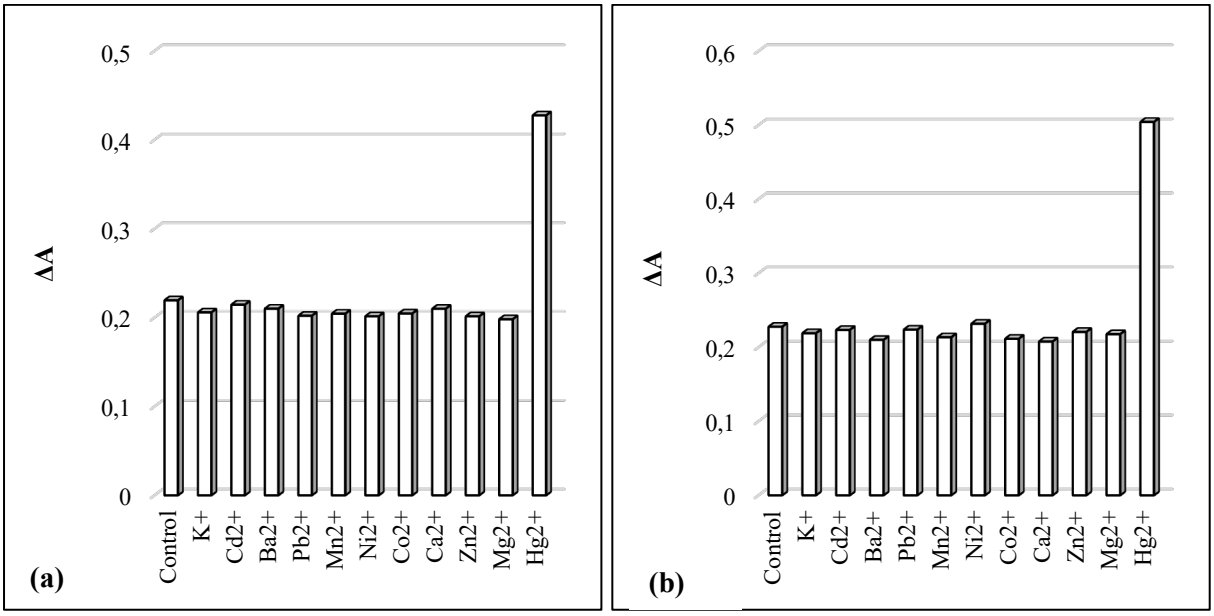

Figure 10. The selectivity of **(a)** AgNPs and **(b)** L-cysteine-capped AgNPs

Table 3. The recovery values of the metal cations for AgNPs and L-cysteine-capped AgNPs

Metal cations	Recovery (R %)	
	AgNPs	L-cysteine-capped AgNPs
K^{+}	93.18	96.18
Cd^{2+}	97.54	98.11
Ba^{2+}	95.29	92.22
Pb^{2+}	91.27	98.29
Mn^{2+}	92.48	93.76
Ni^{2+}	90.97	101.80
Co^{2+}	92.58	92.88
Ca^{2+}	95.24	91.21
Zn^{2+}	90.97	96.92
Mg^{2+}	89.32	95.61

The colorimetric Hg^{2+} detection performances of the synthesized nanomaterials were examined with the use of various water samples such as drinking water, tap water, treated tap water, and distilled water via standard recovery method. Accordingly, different Hg^{2+} concentrations were spiked into the water samples, and the experiments of the colorimetric Hg^{2+} detection were carried out in regards to the method given in Material and Method subsection 2.2. The obtained absorbance differences were converted to concentrations using the calibration lines in the related Hg^{2+} concentration range [2]. The recovery values were calculated with Equation 3 given below:

$$\text{Recovery \% (R \%)} = \frac{\text{Experimental } Hg^{2+} \text{ concentration value}}{\text{Theoretical } Hg^{2+} \text{ concentration value}} \text{ x } 100 \qquad (3)$$

The calculated recovery values given in Table 4 ranged between 91.85 and 110 % for AgNPs while they were between 96 and 109.46 % for L-cysteine-capped AgNPs. Accordingly, the recovery values proved better performance of L-cysteine-capped AgNPs for the colorimetric Hg^{2+} detection in the real water samples, which showed the negligible effect of other interfering agents in the real samples on the validation of the method.

Table 4. The experimental concentrations and the recovery values of AgNPs and L-cysteine-capped AgNPs for real water samples

Real water sample	Theoretical concentration (µM)	AgNPs		L-cysteine-capped AgNPs	
		Experimental concentration (µM)	R %	Experimental concentration (µM)	R %
Drinking water	10	9.82±0.17	98.20	9.77±0.13	97.73
	40	40.79±0.15	101.98	39.42±0.11	98.54
	200	206.20±0.21	103.10	204.78±0.19	102.39
Tap water	10	9.18±0.44	91.85	9.72±0.31	97.22
	40	41.91±0.19	104.78	38.40±0.12	96.00
	200	215.42±0.66	107.71	216.54±0.43	108.27
Treated tap water	10	11.00±0.35	110.00	10.95±0.26	109.46
	40	41.75±0.15	104.38	38.62±0.08	96.54
	200	215.66±0.71	107.83	217.84±0.54	108.92
Distilled water	10	10.82±0.22	108.15	10.88±0.17	108.79
	40	40.79±0.18	101.98	39.71±0.14	99.27
	200	211.01±0.52	105.51	193.38±0.41	96.69

4. Conclusions

The favorable green synthesis of nanomaterials under mild conditions for various applications is still in demand both industrially and environmentally in regards to saving energy, operating safely, and avoiding the use of hazardous chemicals. From this point of view, this study has reported the results of the green synthesis of AgNPs and L-cysteine-capped AgNPs using *F. vulgare* seed extract as the reducing agent in a simple, environmentally friendly, and efficient route for the colorimetric Hg^{2+} detection. L-cysteine was used as a capping agent in the synthesis of the nanomaterials and the obtained results were evaluated in terms of the effect of L-cysteine use on the nanomaterial structure and colorimetric detection. The characterization results showed that L-cysteine was capped successfully on AgNPs and L-cysteine-capped AgNPs exhibited higher crystallinity and improved monodispersity. Thus, the enhanced properties of L-cysteine-capped AgNPs provided better colorimetric Hg^{2+} detection. Accordingly, L-cysteine-capped AgNPs had lower minimum detection limit value than that of AgNPs ($LOD_{L\text{-cysteine-capped AgNPs}}$=0.36 µM<$LOD_{AgNPs}$=1.58 µM). In the studies of selectivity and applicability in real waters, the recovery values of L-cysteine-capped AgNPs exhibited lower variation than that of AgNPs, which indicated that L-cysteine-capped AgNPs could be used more effectively in presence of various metal cations and other interfering agents in the real samples. In this study, for the first time in the literature, L-cysteine-capped AgNPs were synthesized using *F. vulgare* seed extract and utilized as a sensor for the colorimetric Hg^{2+} detection. Unlike some reported studies of the colorimetric Hg^{2+} detection where hazardous chemicals have been used for the synthesis of nanomaterial, this study offered a practical approach to the synthesis of selective, sensitive, and applicable colorimetric sensor of L-cysteine-capped AgNPs by converting a green resource (*F. vulgare*) into economic value.

Ethics in Publishing

There are no ethical issues regarding the publication of this study.

References

[1] Aminu, A., Oladepo, S. A., (2021) Fast Orange Peel-Mediated Synthesis of Silver Nanoparticles and Use as Visual Colorimetric Sensor in the Selective Detection of Mercury(II) Ions. Arabian Journal for Science and Engineering, 46 (6) 5477–5487.

[2] Muhammad, S. P., Shah, M. R., Ullah, R., Ahmad, I., Ali, K., (2022) Synthesis and Characterization of Functionalized Silver Nanoparticles for Selective Screening of Mercury (II) Ions. Arabian Journal for Science and Engineering, 47 (6) 7135–7145.

[3] Jayeoye, T. J., Eze, F. N., Olatunji, O. J., Tyopine, A. A., (2022) Synthesis of biocompatible Konjac glucomannan stabilized silver nanoparticles, with Asystasia gangetica phenolic extract for colorimetric detection of mercury (II) ion. Scientific Reports, 12 (1) 1–15.

[4] Kumar, P., Sonkar, P. K., Tiwari, K. N., Singh, A. K., Mishra, S. K., Dixit, J., Ganesan, V., Singh, J., (2022) Sensing of mercury ion using light induced aqueous leaf extract mediated green synthesized silver nanoparticles of Cestrum nocturnum L. Environmental Science and Pollution Research, 29 (53) 79995–80004.

[5] Khwannimit, D., Jaikrajang, N., Dokmaisrijan, S., Rattanakit, P., (2019) Biologically green synthesis of silver nanoparticles from Citrullus lanatus extract with L-cysteine addition and investigation of colorimetric sensing of nickel(II) potential. Materials Today: Proceedings, 17 2028–2038.

[6] Avissa, M., Alauhdin, M., (2022) Selective Colorimetric Detection of Mercury(II) Using Silver Nanoparticles-Chitosan. Molekul, 17 (1) 107–115.

[7] Kumar, K. S., Ramakrishnappa, T., (2021) Green synthesized uncapped Ag colloidal nanoparticles for selective colorimetric sensing of divalent Hg and H2O2. Journal of Environmental Chemical Engineering, 9 (4) 105365.

[8] Taşkıran, F., Uzunoğlu, D., Özer, A., (2017) Biosynthesis, Characterisation and Determination of Adsorbent Properties of Silver Nanoparticles With Cyprus Acacia (Acacia Cyanophylla) Leaf Extract. Anadolu University Journal Of Science And Technology A - Applied Sciences and Engineering, 1–1.

[9] Chen, J., Ding, J., Li, D., Wang, Y., Wu, Y., Yang, X., Chinnathambi, A., Salmen, S. H., Ali Alharbi, S., (2022) Facile preparation of Au nanoparticles mediated by Foeniculum Vulgare aqueous extract and investigation of the anti-human breast carcinoma effects. Arabian Journal of Chemistry, 15 (1) 103479.

[10] Shrivas, K., Sahu, B., Deb, M. K., Thakur, S. S., Sahu, S., Kurrey, R., Kant, T., Patle, T. K., Jangde, R., (2019) Colorimetric and paper-based detection of lead using PVA capped silver nanoparticles: Experimental and theoretical approach. Microchemical Journal, 150 (August) 104156.

[11] Vyas, G., Bhatt, S., Paul, P., (2019) Synthesis of calixarene-capped silver nanoparticles for colorimetric and amperometric detection of mercury (Hg II , Hg 0). ACS Omega, 4 (2) 3860–3870.

[12] Sharma, P., Mourya, M., Choudhary, D., Goswami, M., Kundu, I., Dobhal, M. P., Tripathi, C. S. P., Guin, D., (2018) Thiol terminated chitosan capped silver nanoparticles for sensitive and selective detection of mercury (II) ions in water. Sensors and Actuators, B: Chemical, 268 310–318.

[13] Cheon, J. Y., Park, W. H., (2016) Green synthesis of silver nanoparticles stabilized with mussel-inspired protein and colorimetric sensing of lead(II) and copper(II) ions. International Journal of Molecular Sciences, 17 (12)

[14] Chugh, D., Viswamalya, V. S., Das, B., (2021) Green synthesis of silver nanoparticles with algae and the importance of capping agents in the process. Journal of Genetic Engineering and Biotechnology, 19 (1)

[15] Poosinuntakul, N., Parnklang, T., Sitiwed, T., Chaiyo, S., Kladsomboon, S., Chailapakul, O., Apilux, A., (2020) Colorimetric assay for determination of Cu (II) ions using L-cysteine functionalized silver nanoplates. Microchemical Journal, 158 (April) 105101.

[16] Maiti, S., Barman, G., Konar Laha, J., (2016) Detection of heavy metals (Cu+2, Hg+2) by biosynthesized silver nanoparticles. Applied Nanoscience (Switzerland), 6 (4) 529–538.

[17] Perni, S., Hakala, V., Prokopovich, P., (2013) Biogenic synthesis of antimicrobial silver nanoparticles capped with L-cysteine. Colloids and Surfaces A: Physicochemical and Engineering Aspects, 460 219–224.

[18] Novoa, C. C., Tortella, G., Seabra, A. B., Diez, M. C., Rubilar, O., (2022) Cotton Textile with Antimicrobial Activity and Enhanced Durability Produced by L-Cysteine-Capped Silver Nanoparticles. Processes, 10 (5)

[19] Zhang, W., Zhang, L., Sun, Y., (2015) Size-controlled green synthesis of silver nanoparticles assisted by L-cysteine. Frontiers of Chemical Science and Engineering, 9 (4) 494–500.

[20] Qingquan, G., Xinfu, M., Yu, X., Wei, T., Hui, Z., (2017) Green synthesis and formation mechanism of Ag nanoflowers using L-cysteine and the assessment of Ag nanoflowers as SERS substrates. Colloids and Surfaces A: Physicochemical and Engineering Aspects, 530 (June) 33–37.

[21] Memon, R., Memon, A. A., Sirajuddin., Balouch, A., Memon, K., Sherazi, S. T. H., Chandio, A. A., Kumar, R., (2022) Ultrasensitive colorimetric detection of Hg2+ in aqueous media via green synthesis by Ziziphus mauritiana Leaf extract-based silver nanoparticles. International Journal of Environmental Analytical Chemistry, 102 (18) 7046–7061.

[22] Cao, X., Zhu, L., Yu, G., Zhang, X., Jin, H., He, D., (2023) Visual and colorimetric determination of mercury (II) based on lignosulfonate-capped silver nanoparticles. Green Chemistry Letters and Reviews, 16 (1)

[23] Fan, P., He, S., Cheng, J., Hu, C., Liu, C., Yang, S., Liu, J., (2021) l-Cysteine modified silver nanoparticles-based colorimetric sensing for the sensitive determination of Hg2+ in aqueous solutions. Luminescence, 36 (3) 698–704.

[24] Samuel, V. R., Rao, K. J., (2023) A rapid colorimetric dual sensor for the detection of mercury and lead ions in water using cysteine capped silver nanoparticles. Chemical Physics Impact, 6 (December 2022) 100161.

[25] Irfan, M. I., Amjad, F., Abbas, A., Ur Rehman, M. F., Kanwal, F., Saeed, M., Ullah, S., Lu, C., (2022) Novel Carboxylic Acid-Capped Silver Nanoparticles as Antimicrobial and Colorimetric Sensing Agents. Molecules, 27 (11) 1–13.

[26] Ali, I., Imkan., Ullah, S., Ahmed, F., Yasmeen, S., Imran, M., Althagafi, I. I., Shah, M. R., (2021) Synthesis and characterization of triazole stabilized silver nanoparticles as colorimetric probe for mercury. Colloids and Surfaces A: Physicochemical and Engineering Aspects, 629 (March) 127419.

[27] Plaeyao, K., Kampangta, R., Korkokklang, Y. et al., (2023) Gingerol extract-stabilized silver nanoparticles and their applications: colorimetric and machine learning-based sensing of Hg(ii) and antibacterial properties. RSC Advances, 13 (29) 19789–19802.

[28] Saenchoopa, A., Boonta, W., Talodthaisong, C., Srichaiyapol, O., Patramanon, R., Kulchat, S., (2021) Colorimetric detection of Hg(II) by γ-aminobutyric acid-silver nanoparticles in water and the assessment of antibacterial activities. Spectrochimica Acta - Part A: Molecular and Biomolecular Spectroscopy, 251 119433.

[29] Demirezen Yılmaz, D., Aksu Demirezen, D., Mıhçıokur, H., (2021) Colorimetric detection of mercury ion using chlorophyll functionalized green silver nanoparticles in aqueous medium. Surfaces and Interfaces, 22 (September 2020) 100840.

[30] Kalam, A., Al-Sehemi, A. G., Ashrafuzzaman, M., Sharif, A. M., Yadav, P., Du, G., (2023) Optical and Colorimetric Sensing of Toxic Mercury Ion Using Green Synthesized Silver Nanoparticles. Bulletin of the Chemical Society of Ethiopia, 37 (5) 1287–1298.

[31] Das, A., Bhadra, K., Kumar, G. S., (2011) Targeting RNA by small molecules: Comparative structural and thermodynamic aspects of aristololactam-β-D-glucoside and daunomycin binding to tRNA phe. PLoS ONE, 6 (8)